

Correlation factors for interstitial-mediated self-diffusion in the diamond lattice: Kinetic lattice Monte Carlo approach

Renyu Chen^{1,*} and Scott T. Dunham^{1,2}

¹*Department of Electrical Engineering, University of Washington, Seattle, Washington 98195, USA*

²*Department of Physics, University of Washington, Seattle, Washington 98195, USA*

(Received 1 January 2011; revised manuscript received 11 March 2011; published 28 April 2011)

We have performed extensive analysis of the correlation factors for interstitial-mediated self-diffusion via various possible mechanisms and hopping networks in the diamond lattice using the kinetic lattice Monte Carlo approach. The correlation factor for the kick-out mechanism in the tetrahedral hopping network is calculated to be 0.73, in agreement with previous results; and the value for the hexagonal hopping network is 0.47 for the dominant mechanism. For the mechanism where a split interstitial is stable (“stable-split” mechanism), the correlation factor for the tetrahedral network stays the same while that for the hexagonal network increases to 0.62. We then performed simulations for the diffusion process of silicon involving multiple mechanisms. The choice of mechanisms is justified by *ab initio* calculations. We conclude that unlike vacancy diffusion, interstitial self-diffusion has a temperature-dependent correlation factor. This conclusion holds in general for diffusion processes involving multiple mechanisms with different activation energies. The correlation factor obtained from *ab initio* results for interstitial-mediated self-diffusion in silicon at 1000–1100 °C is 0.64–0.80, compared to the value of 0.6 extracted from the experiment.

DOI: 10.1103/PhysRevB.83.134124

PACS number(s): 66.30.–h, 61.72.jj

I. INTRODUCTION

Self-diffusion is the most fundamental process in crystals. Under intrinsic conditions, it is caused by point defects such as vacancies and interstitials. Experimentally, self-diffusion is usually measured by the usage of stable isotopes as tracers. Assuming the diffusion correlation factors of all charge states are equal,^{1,2} the tracer diffusivity can be related to the self-diffusion coefficients via^{3–5}

$$D_T = f_I D_I \frac{C_I^*}{C_S} + f_V D_V \frac{C_V^*}{C_S}. \quad (1)$$

The symbols f , D , and C^* on the right-hand side denote the diffusion correlation factors, the diffusivity of interstitials (I) and vacancies (V), and the equilibrium concentrations, respectively. C_S is the concentration of the native lattice atom. The correlation factor enters the equation because although the movement of the point defects alone can be treated as uncorrelated random walks, the successive jumps of a tracer atom are correlated, due to interactions with intrinsic point defects.^{5,6} The correlation factor is generally different for different crystals. In this paper, we limit our analysis to the diamond lattice structure, with representative materials including the group IV elements (C, Si, Ge, α -Sn, and Pb). In the diamond lattice, the correlation factor for the vacancy-mediated self-diffusion was calculated to be 0.5 by Compaan and Haven⁷ using electric network theory. Since the vacancy mechanism is simple and only involves the vacancy-silicon exchange, this value is widely accepted.³ However, the situation is much more complicated when it comes to the correlation factor for interstitial-mediated diffusion, since there are many possible mechanisms. In another paper,⁶ Compaan and Haven also calculated the correlation factor for interstitial diffusion as 0.7273, assuming a tetrahedral configuration for interstitials and a kick-out mechanism. However, their analysis is limited to just one interstitial configuration, and the process

of constructing and appropriately truncating resistive networks is quite tedious.

Over the past 50 years, due to the pervasive applications of silicon technology, the self-diffusion phenomenon in silicon has been investigated by many researchers. Experimental data⁸ show that the value of f_I must be about 0.6 in order to match phosphorus diffusion data in silicon. Meanwhile, various *ab initio* investigations on self-diffusion in silicon report values of 0.56,⁹ 0.59,¹⁰ 0.69,¹⁰ and 0.75.¹¹ Generally, for a simple mechanism, the correlation factor depends only on the geometric aspects of the hopping transitions. However, for real situations such as interstitial self-diffusion in silicon, where multiple mechanisms are present, the correlation factor also depends on the energetics of the formation and migration of the interstitial defects. In this paper, we have first performed extensive analysis of various possible mechanisms and hopping networks of interstitial self-diffusion in the diamond lattice. We then identify the possible mechanisms involved in self-diffusion in silicon based on *ab initio* calculation results and calculate the effective correlation factor for the combined diffusion mechanism in silicon.

II. NUMERICAL DETAILS

According to the statistical diffusion theory,^{12–14} the tracer diffusion correlation factor is related to the square displacements of the tracer and interstitial by

$$f = \frac{\overline{(\Delta r^2/N)^{tr}}}{\overline{(\Delta r^2/N)^I}}, \quad (2)$$

where the superscripts tr and I denote tracer and interstitial properties, respectively. Δr^2 and N are the square displacement and total hopping steps. For a single mechanism in a given hopping network, the quantity on the right-hand side of Eq. (2)

can be calculated by the average cosine value of the angles between successive jumps:

$$f = \frac{1 + 2\overline{\cos\theta}_{i,i+1}^{tr} + 2\overline{\cos\theta}_{i,i+2}^{tr} + \dots}{1 + 2\overline{\cos\theta}_{i,i+1}^I + 2\overline{\cos\theta}_{i,i+2}^I + \dots} \quad (3)$$

For the mechanisms discussed below, all of the nonsuccessive jumps are uncorrelated (i.e., $\overline{\cos\theta}_{i,j} = 0$, for $j > i + 1$). Besides, half of the successive jumps are also uncorrelated (i.e., $\overline{\cos\theta}_{i,i+1} = 0$, for every second i). Therefore, we can simplify Eq. (3) as⁶

$$f = \frac{1 + \overline{\cos\theta}^{tr}}{1 + \overline{\cos\theta}^I}, \quad (4)$$

where the $\overline{\cos\theta}$ terms without subscripts (i) denote the averages of the nonzero cosine values corresponding to the angles between the vectors of correlated hops.

To carry out simulation of the diffusion process of tracers and interstitials, we have used the kinetic lattice Monte Carlo (KLMC) approach,^{15–18} which ignores atomic vibrations and treats diffusion as stochastic transitions between locally metastable states. By replicating the sequence of atomic transitions and arrangements, this approach can directly simulate the diffusion process on the atomic level while still achieving macroscopic system sizes and practical time scales.^{19,20}

The simulation domain consists of a three-dimensional array of native lattice atoms. We have performed tests on different domain sizes and found that the influence of the domain size on the results is negligible. Periodic boundary conditions are used, but the times of crossing through periodic boundaries are included in the calculation of displacements. At any step, there are several possible interstitial hops with rates determined by the associated vibration frequencies and migration energies. At each step, a hop is chosen with the probability weighted by the associated hopping rates. After each hop, the position of the atom is updated, and rates are recalculated.^{19–21}

Since the correlation factor does not depend on tracer concentration, we have used in our simulation only one tracer, which starts off at an interstitial site²² and move randomly in the domain. We also track the trajectory of the interstitial, which is just the extra atom (either a tracer or a native atom) in the domain. For a single mechanism in a given hopping network, we use Eq. (4) to calculate the correlation factor. For combined mechanisms, Eq. (2) is used; and the ratio is determined via a linear fit to the Δr^2 -versus- N data.

All the *ab initio* calculations were done using the density functional theory (DFT) code VASP,^{23,24} with the Perdew-Wang 1991 generalized gradient approximation functional²⁵ and ultrasoft Vanderbilt-type pseudopotentials.^{26,27} All calculations were performed in a nominally 64-atom supercell with periodic boundary conditions and $2 \times 2 \times 2$ Monkhorst-Pack k -point sampling. Calculations have also been carried out for 216-atom supercells and the change of total energy differences is within 0.02 eV. An energy cutoff of 250 eV was used to achieve required accuracy. The structures were fully relaxed to a maximal force of less than 0.005 eV/Å per atom. The climbing image nudged elastic band (NEB) method^{28,29} was used to identify transition paths between two given stable

configurations, with the stopping criterion being a maximum force less than 0.005 eV/Å per atom for each image.

III. CORRELATION FACTOR OF THE KICK-OUT MECHANISM

Over the past years, many interstitial self-diffusion mechanisms have been proposed. Some argue a direct mechanism, in which interstitials make a sequence of direct hops between interstitial sites. In this case, the tracer and the interstitial are always the same atom, and the jumps will, in general, be uncorrelated.⁶ Another set of mechanism involves atoms on lattice sites and is called the indirect kick-out mechanism.³⁰ In this mechanism, a tracer atom on an interstitial site A approaches a native atom at the lattice site B and kicks it out onto an interstitial site C , after which the tracer takes the lattice site B . If we think of the split-interstitial I_x as the intermediate state, the kick-out process actually consists of two processes: $I_i \rightarrow I_x$ and $I_x \rightarrow I_i$. In this kick-out process, the tracer has made one hop from A to B ; while the interstitial has made two successive hops, from A to B and then to C . This kick-out mechanism assumes that the processes $I_i \rightarrow I_x$ and $I_x \rightarrow I_i$ happen in cascades. This kick-out mechanism will generally be correlated since, in the next move of the tracer on site B , it will have a higher probability of being kicked back by the new interstitial atom nearby (on site C). Once the tracer atom is kicked out again to an interstitial site, the next step will generally be uncorrelated with the previous step. Thus, by tracking the average cosine values of the incoming and outgoing hop directions during the kick-out processes, we can determine the correlation factor via Eq. (4).

Compaan and Haven⁶ determine the $\overline{\cos\theta}$ values in Eq. (4) for the kick-out mechanism using resistive network theory and calculate the correlation factor to be 0.7273 for the tetrahedral network ($I_t \leftrightarrow I_x \leftrightarrow I_t$). Apart from considering the tetrahedral network, we extend the analysis to include the hexagonal network, as both tetrahedral and hexagonal interstitials have been reported in various DFT studies as the low-energy structures in silicon and germanium.^{31–34} Consider a typical kick-out process where an interstitial atom kicks a native atom on the lattice site out onto a new interstitial site. In the tetrahedral network, shown in Fig. 1(a), the tracer atom starts at one of the tetrahedral sites t_0 and kicks the silicon atom onto one of the neighboring interstitial sites t_i ($i = 1, 2, 3$). During this process, the tracer moves from t_0 to the lattice site; while the interstitial moves from t_0 to t_i . Due to symmetry, these three t_i sites are equivalent, with $\overline{\cos\theta}^I$ equal to 1/3. In the hexagonal hopping network, shown in Fig. 1(b), the tracer atom starts at one of the interstitial sites h_0 and kicks the silicon atom onto one of the neighboring interstitial sites h_i ($i = 1, 2, \dots, 9$) on the other side of the lattice site (three sites have been excluded since they are on the same side as h_0). We break the possible hexagonal destinations into three groups, with $\overline{\cos\theta}^I$ equal to 9/11, 7/11, and 1/11, respectively. Correspondingly, we have three submechanisms for the hexagonal hopping network. We argue that for geometry reasons the mechanism with $\overline{\cos\theta}^I = 9/11$ is the dominant process, which is also supported by *ab initio* calculations. For the sake of completeness, we include all three submechanisms in our analysis.

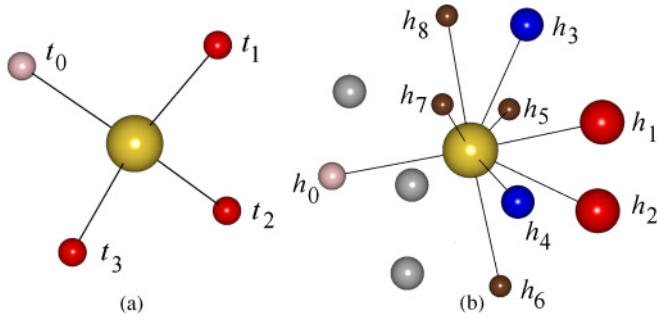


FIG. 1. (Color online) Schematics of the kick-out mechanism in the (a) tetrahedral and (b) hexagonal networks. t_0 and h_0 denote the incoming tracer. The center atom is the silicon atom being kicked out. For tetrahedral configurations t_{1-3} (red/dark spheres) are equivalent, while for hexagonal configurations, the neighbors can be divided into three groups: $h_{1,2}$ (red/dark, large spheres), $h_{3,4}$ (blue/dark, medium spheres), and h_{5-8} (brown/dark, small spheres). The other h sites (gray/light, medium spheres) are excluded.

We have calculated the correlation factor values for the kick-out mechanism in the tetrahedral and hexagonal networks. The results are listed in Table I. The value for the tetrahedral network (0.7276 ± 0.0001) is very close to Compaan and Haven’s value (0.7273).⁶ Actually we believe that our value is more accurate than Compaan and Haven’s which is derived from truncating infinite resistive networks. This result demonstrates the validity of the KLMC approach. The value for the hexagonal hopping network decreases as $\cos \theta^I$ increases. For all the mechanisms, the $\overline{\cos \theta^{tr}}$ values are negative, consistent with the argument that after the tracer kicks out an atom, it will have a higher probability of being kicked back.

IV. CORRELATION FACTOR OF THE STABLE-SPLIT MECHANISM

The above analysis assumes that the $I_i \rightarrow I_x$ and $I_x \rightarrow I_i$ processes happen in cascades, which implies that the transition state, which is the split-interstitial configuration, is unstable. However, it has been proposed based on various *ab initio* results that there exists a stable split interstitial oriented along the $\langle 110 \rangle$ direction.³⁴ Therefore, in this part we drop the assumption of the kick-out mechanism and consider the situation where the split-interstitial is stable (denoted as the

TABLE I. Correlation factors for the kick-out mechanism in the tetrahedral and hexagonal hopping networks. The mechanism in the hexagonal network is categorized into three groups based on the kick-out direction. The parentheses denote the corresponding destinations after the kick-out. The $\cos \theta^I$ value is fixed for each mechanism, and the $\overline{\cos \theta^{tr}}$ value is calculated from the KLMC approach. The uncertainty of the correlation factor is the standard error of the mean.

Network	$\overline{\cos \theta^I}$	$\overline{\cos \theta^{tr}}$	f
Tetrahedral (t_{1-3})	4/12	-0.0299	0.7276 ± 0.0001
Hexagonal ($h_{1,2}$)	9/11	-0.1475	0.4690 ± 0.0001
Hexagonal ($h_{3,4}$)	5/11	-0.0731	0.6372 ± 0.0001
Hexagonal (h_{5-8})	1/11	-0.0073	0.9099 ± 0.0001

“stable-split” mechanism hereafter). In this case, either of the atoms comprising the split can hop onto neighboring interstitial sites. In turn, the atom on interstitial sites can hop onto a lattice site and form a split interstitial with the lattice atom.

We again consider the tetrahedral and hexagonal hopping networks. For split interstitials, we limit our analysis to $\langle 110 \rangle$ -split interstitials, which have been found to be the most stable structure in Si and Ge.³⁴ Due to the fact that the $\langle 110 \rangle$ -split interstitial has an orientation, certain orientation constraints have to be imposed on the migration paths. Figure 2 illustrates the constraints for the split hopping onto tetrahedral and hexagonal sites. By intuition we can see that only the sites that are located along the direction most aligned with the split orientation are favored [t_B in Fig. 2(a) and h_C in Fig. 2(b)]. The others are located in a roughly orthogonal [t_A in Fig. 2(a) and h_A, h_B, h_D in Fig. 2(b)] direction and are therefore unfavorable. Similarly, when a tetrahedral (hexagonal) interstitial hops onto the lattice site and forms a split interstitial, only three (two) out of the six $\langle 110 \rangle$ -split orientations are allowed. These orientation constraints are verified by the migration barrier results from NEB calculations.

We have calculated the correlation factor values for the stable-split mechanism in the tetrahedral and hexagonal networks with the above orientation constraints imposed. The results are listed in Table II. Using statistical diffusion theory, the $\overline{\cos \theta^I}$ value can be calculated analytically by constructing allowed hopping networks of the interstitial. The average cosine values become smaller than the kick-out mechanism due to the fact that here more choices of $I_x \rightarrow I_i$ hop directions are allowed after an $I_i \rightarrow I_x$ hop. In other words, not only “kick-out” but also “bounce-back” are allowed. The correlation factor for the tetrahedral network is the same as the previous value, simply because when the tracer is bounced back, it returns to the previous interstitial site and has no net displacement, giving no contribution to the total correlation effect. The situation is different for hexagonal sites, since when bounced back, the tracer atom can be on a different interstitial

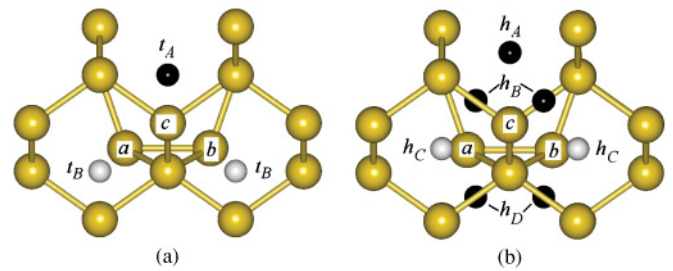


FIG. 2. (Color online) Allowed hopping directions in the (a) split-tetrahedral and (b) split-hexagonal networks, viewed along the $\langle 110 \rangle$ direction. a and b form the $\langle 110 \rangle$ -split interstitial. c is the original lattice site. In (a) the small spheres denote the four first nearest tetrahedral neighbors of the split categorized into two groups, two in t_A and two in t_B . The allowed hopping destinations of the split are the two t_B sites only. In (b) the small spheres denote the 12 first nearest hexagonal neighbors of the split categorized into four groups, two in h_A , four in h_B , four in h_C , and two in h_D . The allowed hopping destinations of the split are the four h_C sites only. Note that some nearest neighbors behind are blocked by the ones in front of them, when viewed along this direction.

TABLE II. Correlation factor values for the tetrahedral and hexagonal hopping networks. The $\overline{\cos\theta^l}$ value is calculated analytically, and the $\overline{\cos\theta^{lr}}$ value is calculated via the KLMC approach. The uncertainty of the correlation factor is the standard error of the mean.

Network	$\overline{\cos\theta^l}$	$\overline{\cos\theta^{lr}}$	f
Tetrahedral	$-1/3$	-0.5150	0.7275 ± 0.0001
Hexagonal	$-1/11$	-0.4357	0.6207 ± 0.0001

site [e.g. in Fig. 2(b) jumping between two h_C sites on the left via atom a].

V. CORRELATION OF COMBINED MECHANISMS IN SILICON

In this part, we perform a case study for interstitial-mediated self-diffusion in silicon. The lowest-energy structures as well as the migration barriers of self-interstitials in silicon have been studied extensively.^{31–34} The general consensus is that the hexagonal, tetrahedral, and $\langle 110 \rangle$ -split interstitials have relatively lower formation energies than other configurations.³⁴ We have performed *ab initio* calculations which confirmed that the lowest-energy structures are the $\langle 110 \rangle$ -split and hexagonal interstitials, with formation energies of 3.70 and 3.79 eV, respectively; while the tetrahedral interstitial has a slightly higher formation energy of 3.97 eV. Using the NEB method, we have identified several migration paths and calculated the associated barriers, which are listed in Table III. The tetrahedral interstitial is found to be an intermediate state, which relaxes to a hexagonal interstitial. The direct (uncorrelated) mechanism, $I_h \leftrightarrow I_h$ via I_t , has a lower barrier than the indirect mechanism $I_x \leftrightarrow I_h$. Previously a fourfold interstitial defect has been reported.³⁵ However, due to the high migration barrier of the concerted exchange,³³ they are less likely to migrate and thus not included in our analysis. The +2 charge state interstitials reported in a recent paper³⁶ are also excluded due to their high migration barriers.

From the analysis above, there are two major hopping mechanisms for self-diffusion in silicon: $I_h \leftrightarrow I_x$, and $I_h \leftrightarrow I_h$. The former is the indirect mechanism in the hexagonal hopping network. The latter is the direct mechanism, with a correlation factor of 1. In the presence of both mechanisms, the hexagonal interstitial can diffuse either directly or indirectly. If we denote the corresponding probabilities as P_{direct} and P_{indirect} , then we have $P_{\text{direct}} = 1 - P_{\text{indirect}}$ and the effective correlation factor f_{eff} should be a function of P_{direct} . To determine the relationship between f_{eff} and P_{direct} , we have

TABLE III. Table III. Migration barriers of various migration paths of interstitials in silicon.

Migration path	Forward barrier (eV)	Reverse barrier (eV)
$I_x \leftrightarrow I_h$	0.34	0.25
$I_x \leftrightarrow I_t$	0.38	0.11
$I_h \leftrightarrow I_h$	0.17	0.17
$I_h \leftrightarrow I_t$	0.17	0.00

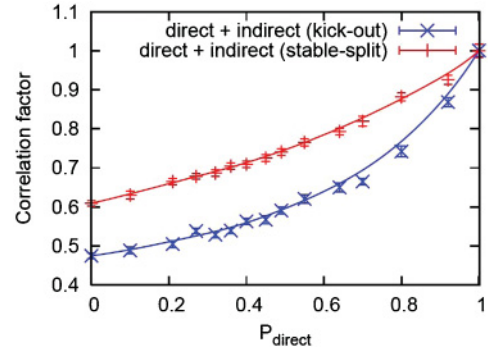


FIG. 3. (Color online) Effective correlation factors of interstitial-mediated self-diffusion in silicon as a function of the probability of hopping via the direct mechanism.

performed KLMC simulations with P_{direct} varying from 0 (pure indirect) to 1 (pure direct). The f_{eff} value is extracted via Eq. (2). For the indirect mechanism, we consider the dominant kick-out mechanism with $\overline{\cos\theta^l} = 9/11$ ($f = 0.4690$) and the stable-split mechanism ($f = 0.6207$). The results are plotted in Fig. 3. As can be seen, the total effective correlation factor increases monotonically as the probability of direct mechanism increases, with values approaching unity when the direct mechanism is more favorable, rendering the diffusion more uncorrelated. The correlation factor for the stable-split mechanism is higher than for the kick-out mechanism for a given P_{direct} . The actual correlation factor for a certain P_{direct} value should lie somewhere between the two curves when the kick-out and stable-split mechanisms are both present.

According to the transition state theory,^{12–14} the probability P_{direct} can be expressed as

$$P_{\text{direct}} = \frac{\Omega_{\text{direct}} \exp(-E_{\text{direct}}^m/kT)}{\Omega_{\text{direct}} \exp(-E_{\text{direct}}^m/kT) + \Omega_{\text{indirect}} \exp(-E_{\text{indirect}}^m/kT)}, \quad (5)$$

where Ω is the entropy factor associated with the mechanisms, and E^m is the corresponding migration barrier. Once the migration barriers are determined, the only variable that controls the probability P_{direct} , and therefore f_{eff} , is the temperature. Therefore, unlike in vacancy diffusion, here the effective correlation factor for the combined mechanisms of interstitial-mediated self-diffusion in silicon is temperature dependent, which may be the reason for the different correlation values reported in literature.^{8–11} Assuming that the entropy factors are the same for the two mechanisms, the correlation factor at 1000–1100 °C is calculated to be 0.64 for the kick-out mechanism and 0.80 for the stable-split mechanism using the values in Table III. This estimate is higher than the reported experimental value of 0.6 for the same temperature range.⁸ Sources for the differences include uncertainties in values extracted experimentally and the energetics of the mechanisms predicted by the DFT calculations which results in overestimation of the probability of the direct mechanism. Another possible source of error comes from the neglect of the entropy difference of the two mechanisms. Better

quantification of the entropy factors requires *ab initio* studies of the vibrational frequencies of the transition states of the two mechanisms.

VI. CONCLUSION

Using the kinetic lattice Monte Carlo approach, we have performed extensive analysis of the correlation factor values of interstitial self-diffusion for various possible mechanisms and hopping networks in the diamond lattice. The correlation factor for the kick-out mechanism in the tetrahedral hopping network is 0.72, which is in agreement with previous results; and the value for the hexagonal hopping network is 0.47 for the dominant mechanism. For the mechanism where a split interstitial is stable (stable-split mechanism), the correlation factor for the tetrahedral network stays the same while that for the hexagonal network increases to 0.62. We then identify the possible mechanisms involved in interstitial-mediated

self-diffusion in silicon based on *ab initio* calculation results and calculate the effective correlation factor for the combined mechanism. Unlike vacancy diffusion, interstitial-mediated self-diffusion has a temperature-dependent correlation factor. This conclusion in general holds for diffusion processes involving multiple mechanisms with different activation energies. The correlation value obtained from *ab initio* results at 1000–1100 °C is 0.64–0.80, higher than the experimental value of 0.6.

ACKNOWLEDGMENTS

This work was partially funded by support from Sony Corporation, Semiconductor Research Corporation, and Micron. The calculations used a computing cluster provided via donations from Intel, AMD, and NSF Grant No. EIA-0101254, as well as EMSL computational resources at the Pacific Northwest National Lab.

*renyu@uw.edu

¹H. Bracht, *Nucl. Instrum. Methods Phys. Res., Sect. B* **253**, 105 (2006).

²H. Bracht, H. H. Silvestri, I. D. Sharp, and E. E. Haller, *Phys. Rev. B* **75**, 035211 (2007).

³A. Seeger and K. P. Chik, *Phys. Status Solidi* **29**, 455 (1968).

⁴U. Gosele and T. Y. Tan, in *Defects in Semiconductors II*, edited by S. Mahajan and J. W. Corbett, MRS Symposia Proceedings No. 14 (Materials Research Society, Pittsburgh, 1983), p. 45.

⁵P. Pichler, *Intrinsic Point Defects, Impurities, and Their Diffusion in Silicon* (Springer, Vienna, 2004).

⁶K. Compaan and Y. Haven, *Trans. Faraday Soc.* **54**, 1498 (1958).

⁷K. Compaan and Y. Haven, *Trans. Faraday Soc.* **52**, 786 (1956).

⁸V. V. Voronkov and R. Falster, in *Gettering and Defect Engineering in Semiconductor Technology XI*, edited by B. Pichaud, A. Claverie, D. Alquier, H. Richter, and M. Kittler (Trans Tech Publications, Zurich, 2005), Vol. 108-109, p. 1.

⁹M. Posselt, F. Gao, and D. Zwicker, *Phys. Rev. B* **71**, 245202 (2005).

¹⁰M. Posselt, F. Gao, and H. Bracht, *Phys. Rev. B* **78**, 035208 (2008).

¹¹B. Sahli and W. Fichtner, *Phys. Rev. B* **72**, 245210 (2005).

¹²H. Eyring, *J. Chem. Phys.* **3**, 107 (1935).

¹³R. Marcelin, *Ann. Phys.* **3**, 120 (1915).

¹⁴E. Wigner, *Z. Phys. Chem. B* **19**, 203 (1932).

¹⁵M. Bunea and S. T. Dunham, *J. Comput.-Aided Mater. Des.* **5**, 81 (1998).

¹⁶R. Chen and S. T. Dunham, *J. Vac. Sci. Technol. B* **28**(1), C1G18 (2010).

¹⁷S. T. Dunham and C. D. Wu, *J. Appl. Phys.* **78**, 2362 (1995).

¹⁸Z. D. Qin and S. T. Dunham, *Phys. Rev. B* **68**, 245201 (2003).

¹⁹A. F. Voter, in *Radiation Effects in Solids*, edited by K. E. Sickafus and E. A. Kotomin (Springer, NATO Publishing Unit, Dordrecht, The Netherlands, 2005).

²⁰A. Horsfield, S. Dunham, and H. Fujitani, in *Multiscale Modeling of Materials*, edited by V. Bulatov, T. de la Rubia, N. Ghoniem,

E. Kaxiras, and R. Phillips, MRS Symposia Proceedings No. 538 (North Holland, Pittsburgh, 1999), p. 285.

²¹Z. D. Qin, Ph.D. thesis, University of Washington, 2005.

²²It is necessary to clarify “interstitial site” versus “interstitial.” An “interstitial site” is a site that is not a regular diamond lattice site. Some of the high-symmetry interstitial sites are the tetrahedral (*t*) and hexagonal (*h*) sites. An interstitial (*I_i*) is a configuration where an atom occupies an interstitial site. Some common types of interstitials are the tetrahedral interstitial (*I_t*), hexagonal interstitial (*I_h*), and split-interstitial (*I_x*) in which two atoms share a lattice site.

²³G. Kresse and J. Hafner, *Phys. Rev. B* **47**, 558 (1993).

²⁴G. Kresse and J. Furthmüller, *Phys. Rev. B* **54**, 11169 (1996).

²⁵J. P. Perdew, J. A. Chevary, S. H. Vosko, K. A. Jackson, M. R. Pederson, D. J. Singh, and C. Fiolhais, *Phys. Rev. B* **46**, 6671 (1992).

²⁶D. Vanderbilt, *Phys. Rev. B* **41**, 7892 (1990).

²⁷G. Kresse and J. Hafner, *J. Phys.: Condens. Matter.* **6**, 8245 (1994).

²⁸G. Henkelman and H. Jonsson, *J. Chem. Phys.* **113**, 9978 (2000).

²⁹G. Henkelman, B. P. Uberuaga, and H. Jonsson, *J. Chem. Phys.* **113**, 9901 (2000).

³⁰E. Koch and C. Wagner, *Z. Phys. Chem. B-Chem. Elem. Aufbau. Mater.* **38**, 295 (1937).

³¹Y. Bar-Yam and J. D. Joannopoulos, *Phys. Rev. Lett.* **52**, 1129 (1984).

³²P. E. Blochl, E. Smargiassi, R. Car, D. B. Laks, W. Andreoni, and S. T. Pantelides, *Phys. Rev. Lett.* **70**, 2435 (1993).

³³D. Caliste, P. Pochet, T. Deutsch, and F. Lancon, *Phys. Rev. B* **75**, 125203 (2007).

³⁴R. J. Needs, *J. Phys.: Condens. Matter.* **11**, 10437 (1999).

³⁵S. Goedecker, T. Deutsch, and L. Billard, *Phys. Rev. Lett.* **88**, 235501 (2002).

³⁶S. Y. Ma and S. Q. Wang, *Phys. Rev. B* **81**, 193203 (2010).